Plasmon ruler with gold nanorod dimers: utilizing the second-order resonance

Maxim R. Shcherbakov,[1] Anton T. Le,[1] Natalia Dubrovina,[2] Anatole Lupu,[2] and Andrey A. Fedyanin[1,*]

[1]*Faculty of Physics, Lomonosov Moscow State University, Moscow 119991, Russia*

[2]*Univ. Paris-Sud, Institut d'Electronique Fondamentale, UMR 8622, 91405 Orsay Cedex, France*

**Corresponding author: fedyanin@nanolab.phys.msu.ru*

Received December 11, 2014; revised March 1, 2015; accepted March 2, 2015;
posted March 3, 2015 (Doc. ID 225798); published March 30, 2015

The idea of utilizing the second-order plasmon resonance of gold nanorod π-dimers for plasmon rulers is introduced. We report on a qualitatively different dependence of the plasmon resonance shift on the interparticle distance for the first- and second-order longitudinal modes of the nanorods, extending the working range of plasmon rulers up to the distance values of approximately 400 nm. © 2015 Optical Society of America

OCIS codes: (250.5403) Plasmonics; (310.6628) Subwavelength structures, nanostructures; (350.4238) Nanophotonics and photonic crystals.

http://dx.doi.org/10.1364/OL.40.001571

Optical properties of gold nanoparticles have contributed to many areas of science and technology, such as drug delivery [1], cell imaging [2], photothermal therapy [3], and others. In particular, a possibility of measuring nanoscale length utilizing pairs of gold nanoparticles—i.e., plasmonic dimers—was demonstrated [4,5] producing the idea of the so-called plasmon ruler (PR). Operating principles of PRs are based on the fact that the spectral position of the surface plasmon resonance (SPR) of a plasmonic dimer strongly depends on the distance between the particles forming the dimer [6]. This phenomenon makes it possible, e.g., to measure the length of a sub-100-nm macromolecule with gold nanoparticles bound to its ends by measuring the SPR position and comparing it to one of the uncoupled nanoparticles [4]. Tailorable nature of SPR allows flexible tuning of plasmonic dimer optical properties by changing the shape, mutual arrangement, or polarization of the incoming light and, hence, the type of the resonance [7–9]. In PRs, however, the maximum measurable distance is still limited to roughly 100 nm.

Nanorods are one of the frequently used shapes to analyze the physics behind the near-field coupling of plasmonic nanoparticles [10]. One distinguishes between two types of nanorod dimers—the so-called π-dimer and σ-dimer, referring to the analogy from the orientation of coupled atomic p-orbitals. Providing subwavelength field localization in the gap between the inline arranged nanoparticles, the σ-dimer is used in nanoantenna research [11] and applications, such as improved surface-enhanced Raman scattering [12]. The π-dimer, on the other hand, is a system conventionally considered for observation of optical magnetism happening when the free-electron currents are out of phase in the nanorods forming the dimer [13]. Finally, for nanorods long enough, it is possible to excite several longitudinal SPR modes [14]. Nevertheless considered theoretically [15,16], the coupling properties of the higher order resonances were neither provided experimentally so far, nor were they considered as a basis for a qualitatively different PR-type system.

In this contribution, we obtain the dependence of the SPR position λ_0 on the distance between the rods d for a set of π-dimers by means of microspectroscopy of gold nanorod samples and corresponding numerical calculations. The first- (fundamental) and second-order longitudinal dipolar plasmon resonances are considered. It is shown that the $\lambda_0(d)$ dependence for the second-order resonance can be used to form a PR with a working distance range of up to 400 nm. On the contrary, far-field interference effects hinder the possibility of using this system as a PR for the same working range if one considers the first-order resonance.

The aim of the present study is to perform a comparative study of a dimer PR operating at the first- or the second-order dipolar resonances. We designed and fabricated several sets of PR structures with significantly different dimensions of the resonant elements but providing very close resonance frequencies when operating accordingly to the design at the first- (I) or second-order (II) resonances. Gold nanoparticle dimer samples were fabricated using electron-beam lithography with a positive electron resist. All the measured nanostructures were located on the same 0.5-mm-thick fused silica substrate. The nanorods were 50 nm in height, 50 nm in width; their length a and the distance d between the edges of nanorods within the dimer varied from sample to sample and constituted a table of parameters with $a = 50$, 100, 150, 200, 300, 400, and 500 nm, and $d = 50$, 100, 150, 250, 350, 450, and 650 nm. Examples of SEM images are shown in Figs. 1(a)–1(d) for different combinations of $a = 100$ nm, $a = 400$ nm, $d = 50$ nm, and $d = 350$ nm. Each nanostructured area had lateral dimensions of $100\mu\text{m} \times 100$ μm and contained approximately 10^4 periodically arranged nanorod dimers. The separation distance between adjacent dimers was of approximately 1.5 μm; the density of each dimer array was chosen intentionally sparse in order to minimize the interaction effects between the nearest neighbors.

Extinction spectra of gold nanorod dimers were obtained by means of the transmission microspectroscopy technique. Transmission spectra were carried out under normal incidence using a white-light microspecrtoscopy setup with a spectral range from 400 to 1400 nm, a spectral accuracy of 0.8 nm, a focal spot of 50 μm in diameter, and a numerical aperture of the focusing system of 0.04. The illumination polarized perpendicularly to the rods

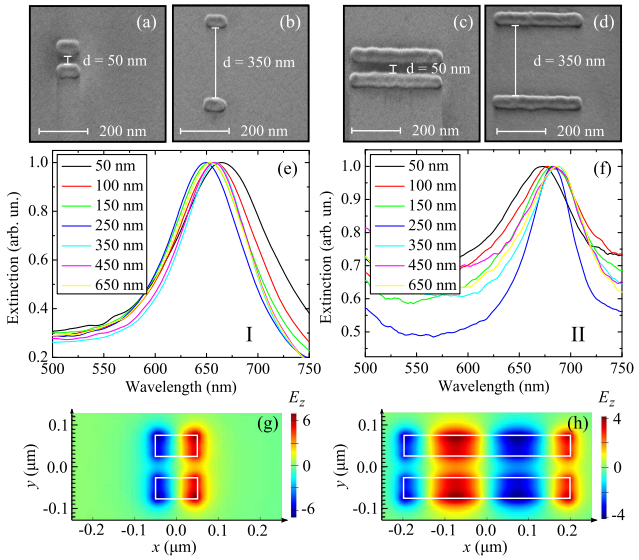

Fig. 1. (a)–(d) SEM micrographs of gold nanorod π-dimers with a nanorod length of $a = 100$ nm or $a = 400$ nm, and an interparticle distance of $d = 50$ nm or 350 nm. (e),(f) Normalized experimental extinction spectra of nanoparticle dimer sets with a nanorod length of 100 nm and 400 nm corresponding to the first- (I) and second-order (II) resonances, respectively. (g),(h) Calculated E_z distribution nearby the nanorod dimers for the first- and second-order longitudinal resonances, respectively, in the cross-section close to the surface of the dimer.

yielded the 1st-order plasmon mode at a wavelength of approximately 550 nm; higher order modes were not observed. As a result, the input polarization state was always set to be parallel to the nanorods.

The transmission spectra of all experimentally studied nanorod dimers were also numerically simulated using the finite-difference time-domain (FDTD) technique. Simulations were performed using FDTD Solutions software from Lumerical Solutions, Inc. Gold [17] nanorods were modeled as cuboids with the width and height fixed at 50 and 30 nm, respectively. The number of grid points per wavelength was set to 22, and an additional 5-nm mesh was implemented in the area of nanorods. The refractive index of the surrounding medium was set to be 1.0 in order to isolate the results from the effects of substrate. The incident electromagnetic field was polarized parallel to the nanorods. Unless otherwise noted, the perfectly matched layer (PML) boundary conditions are implied for each side of the integration volume.

The experimental extinction spectra of the dimer arrays with different interparticle distance d operating at the 1st- and 2nd-order resonances are displayed in the Figs. 1(e) and 1(f), respectively. In a good agreement with the modeling predictions, the resonances are observed around 650 nm for the 100-nm-long rods operating at the 1st-order SPR. For the 400-nm-long rods, which operate at the 2nd-order SPR, the resonance is also found in the same spectral range. The electric field z-projection distribution is represented in Figs. 1(g) and 1(h) indicating the two- and four-antinode structure (standing waves) corresponding to the 1st- and 2nd-order SPRs, respectively.

The extinction spectra displayed in Figs. 1(e) and 1(f) show that the resonance wavelength λ_0 depends on the interparticle separation distance d. This is attributed to the effect of optical coupling between the nanorods. The experimentally observed and numerically calculated variation of the resonance wavelength λ_0 as a function of d for 400-nm- and 500-nm-long nanorods operating at the 2nd-order SPR is shown in Fig. 2. Aside from the 10% difference in the absolute value of resonance wavelength, experimental and modeling results are in good overall agreement.

Sensitivity of λ_0 to d was previously shown to depend on d [18,19]. λ_0 is more sensitive to the variation of d if the latter is small, and less sensitive for larger d values. Comparing the experimentally and numerically attained absolute spectral shifts in the visible $\Delta\lambda$ with those found in literature [5,6] gives about $\Delta\lambda \approx 30$ nm versus $\Delta\lambda \approx 50$ nm, respectively; this is a direct consequence of the large-distance regime picked for the current study. A closer inspection of Fig. 2 reveals that there are some small but persistent deviations between the experimental and modeled results. While the dependence is monotonic up to hundreds of nanometers in the modeled case, it shows some oscillatory behavior in the experiment. The oscillatory-type features in the experimental dependences are a consequence of periodic arrangement of the dimers in a regular 2D array that leads to the diffraction coupling between the nanorods. A similar effect related to the interference between the SPR and diffraction order for a 2D array of nanoantennas was reported in Refs. [20,21]. This effect is discussed in detail in the case of the PR operating at its 1st-order resonance, where its influence is much more dramatic.

Since $\lambda_0(d)$ is oscillatory in both periodic and isolated dimer arrangements, one can calibrate the ruler in the whole range from $d = 0$ to the value where the first derivative of the $\lambda_0(d)$ function becomes equal to zero. This is the range of d that could be subsequently measured with such a ruler, and is thereby referred to as the working range of the PR. In order to access the $\partial\lambda_0(d)/\partial d = 0$ point, we consider the large-d regime, which is in contrast to the small-d regime found in previous descriptions of PRs. To point out the key difference in $\lambda_0(d)$ for the 1st- and 2nd-order resonances, calculations of $\lambda_0(d)$ were carried out for the dimer with $a = 400$ nm for both resonance orders as seen in the left panel of Fig. 3. The working range of the 1st-order-resonance rulers is limited to the value of approximately 170 nm. For $d > 170$ nm, the interparticle far-field effects are believed to disrupt the monotonous dependence

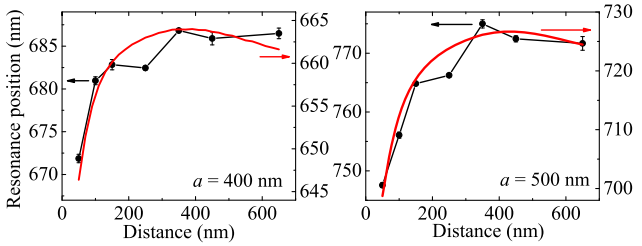

Fig. 2. Measured (connected dots) and calculated (solid curves) position λ_0 of the *second-order* longitudinal dipolar plasmon resonance of nanorod dimers as a function of the interparticle distance d for the sets of 400-nm- and 500-nm-long nanorods.

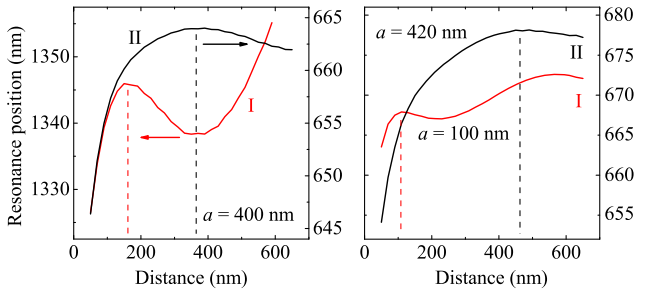

Fig. 3. Calculated position of the 1st-order (I) and 2nd-order (II) longitudinal dipolar plasmon resonances of nanorod dimers as a function of the interparticle distance d: (left) For the nanorods of the same length of $a = 400$ nm, (right) for the nanorods of different lengths of $a = 420$ nm and $a = 100$ nm. Note the right panel having the same scale for both curves. The dashed lines show the upper limit of the PR working range based on the particular dimers.

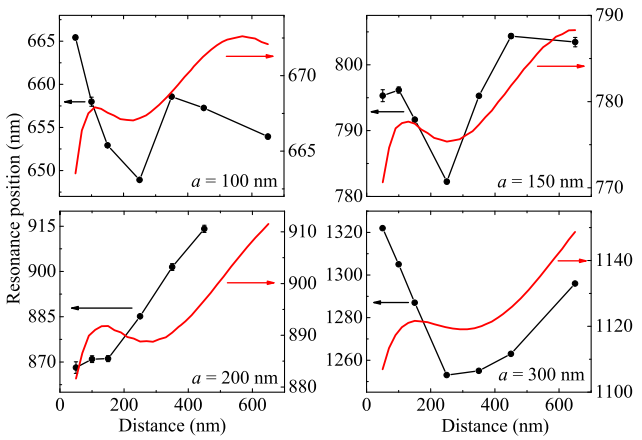

Fig. 4. Measured (connected dots) and calculated (solid curves) position of the *1st-order* longitudinal dipolar plasmon resonance λ_0 of nanorod dimers as a function of the interparticle distance d for the sets of 100-nm-, 150-nm-, 200-nm-, and 300-nm-long nanorods.

leading to a non-monotonous behavior [22]. On the other hand, for the 2nd-order resonance the monotonous growth of the $\lambda_0(d)$ function is extended up to 370 nm. This makes it more beneficial to measure large distance and length values with the 2nd-order resonance of such a ruler. One could argue that the characteristic decay function of $\lambda_0(d)$ scales with the wavelength, and, therefore, it is not feasible to compare graphs in the left panel of Fig. 3. However, the same rule applies if the two resonances are considered on the same wavelength scale as shown in the right panel of Fig. 3. Here, the $\lambda_0(d)$ curves are given for the length values of $a = 420$ nm (2nd-order resonance) and $a = 100$ nm (1st-order resonance). This graph straightforwardly indicates the difference between the 1st- and 2nd-order resonances in plasmonic nanorod dimers. High sensitivity of the 1st-order resonance of a nanoparticle in the presence of the other one is understood—the resonance is "brighter" than the 2nd-order one due to larger polarizability; the overall absolute extinction coefficient of light is approximately 3–4 times larger for the 1st-order resonance than for the 2nd-order one. The same feature of the far-field coupling of dark modes was found in Ref. [20]: darker (quadrupolar) modes of plasmonic cavities are less subject to far-field coupling that the brighter (dipolar) ones.

Another downside of the 1st-order resonance is its dependence on diffraction originating from the periodic arrangement of the dimers. The effect of unwanted diffraction coupling of the 1st-order resonance is demonstrated with the data provided in Fig. 4 for the samples with $a = 100$, 150, 200, and 300 nm. It is seen that for all the samples the shape of the experimental $\lambda_0(d)$ dependence does not reproduce the one obtained in calculations with PML boundary conditions. We assume the substantial mismatch between the experimental and numerical data is connected to the far-field coupling of the dimers in the periodic arrangement. It is therefore natural to compare how the 1st- and 2nd-order resonances behave upon being arranged in arrays of different periods. In order to illustrate the difference of 1st- and 2nd-order resonances in terms of diffraction coupling, the effect of the packing period on extinction is shown in Fig. 5. Here, extinction of the nanorod dimer arrays with $a = 300$ nm and $d = 300$ nm is plotted as a function of wavelength and arrangement period as calculated with FDTD using periodic boundary conditions. It is seen that for the 1st-order resonance located in the infrared part of the spectrum, there is a strong influence of diffraction coupling between the rods. The effect of diffraction on the resonant wavelength of plasmons was reported previously for the 1st-order resonance [21]. As stated above, this effect is not manifested in such a strong fashion for the 2nd-order resonance. One can see that the 2nd-order resonance situated at approximately 600 nm is almost unaffected by the period alteration, and its position is preserved within the uncertainty of about 5 nm. In contrast, the 1st-order resonance is seen to be considerably shifted within the range from 1100 to 1300 nm. The feature of the 2nd-order resonance is advantageous in terms of general stability of the PR to diffraction coupling, which could be critical in PRs allocated in periodical arrangements.

In conclusion, the use of the second-order plasmon resonance in gold nanorod π-dimers for plasmon rulers

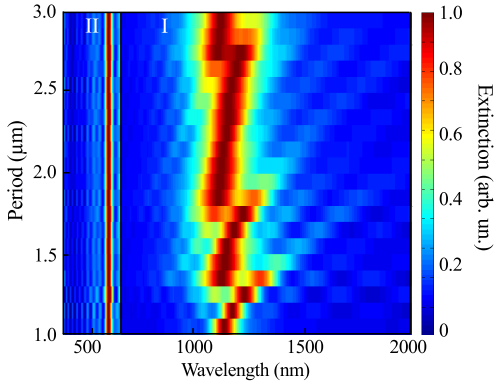

Fig. 5. Normalized calculated extinction spectra of the dimers with $a = d = 300$ nm as a function of the packing period. The 1st-order and the 2nd-order longitudinal dipolar plasmon resonances are indicated with I and II, respectively. For the sake of clarity, the spectra are normalized separately; the border between the two normalization regions at $\lambda = 650$ nm is denoted with a black vertical line.

is justified experimentally and theoretically. Explicit evidences are provided to demonstrate the essential difference between π-dimer nanorod rulers operating at the first- and second-order longitudinal surface plasmon resonances of the nanorods. The maximum distance that can be measured using a ruler operating at the second-order resonance is extended up to 400 nm as compared to about 100 nm provided by the ruler based on the first-order resonance. Moreover, the second-order-resonance ruler is shown to merely suffer from diffraction coupling. This fact makes second-order surface plasmon resonances attractive for periodic-arrangement solutions involving plasmon rulers.

The authors are grateful to the IEF MINERVE cleanroom staff for their help with the samples technological realization and to Denis Presnov for providing SEM micrographs of the samples. This work was supported by Russian Foundation for Basic Research and Ministry of Education and Science of Russian Federation (contract RFMEFI61314X0029).

References

1. S. D. Brown, P. Nativo, J.-A. Smith, D. Stirling, P. R. Edwards, B. Venugopal, D. J. Flint, J. A. Plumb, D. Graham, and N. J. Wheate, J. Am. Chem. Soc. **132**, 4678 (2010).
2. S. D. Perrault and W. C. W. Chan, Proc. Natl. Acad. Sci. **107**, 11194 (2010).
3. X. Huang, I. H. El-Sayed, W. Qian, and M. A. El-Sayed, J. Am. Chem. Soc. **128**, 2115 (2006).
4. B. M. Reinhard, M. Siu, H. Agarwal, A. P. Alivisatos, and J. Liphardt, Nano Lett. **5**, 2246 (2005).
5. P. K. Jain, W. Huang, and M. A. El-Sayed, Nano Lett. **7**, 2080 (2007).
6. W. Rechberger, A. Hohenau, A. Leitner, J. R. Krenn, B. Lamprecht, and F. R. Aussenegg, Opt. Commun. **220**, 137 (2003).
7. C.-Y. Tsai, J.-W. Lin, C.-Y. Wu, P.-T. Lin, T.-W. Lu, and P.-T. Lee, Nano Lett. **12**, 1648 (2012).
8. C. Tabor, R. Murali, M. Mahmoud, and M. A. El-Sayed, J. Phys. Chem. A **113**, 1946 (2009).
9. S.-C. Yang, H. Kobori, C.-L. He, M.-H. Lin, H.-Y. Chen, C. Li, M. Kanehara, T. Teranishi, and S. Gwo, Nano Lett. **10**, 632 (2010).
10. A. M. Funston, C. Novo, T. J. Davis, and P. Mulvaney, Nano Lett. **9**, 1651 (2009).
11. Z. Liu, A. Boltasseva, R. H. Pedersen, R. Bakker, A. V. Kildishev, V. P. Drachev, and V. M. Shalaev, Metamater. **2**, 45 (2008).
12. K. D. Alexander, K. Skinner, S. Zhang, H. Wei, and R. Lopez, Nano Lett. **10**, 4488 (2010).
13. V. A. Podolsky, A. K. Sarychev, and V. M. Shalaev, J. Nonlinear Opt. Phys. Mater. **11**, 65 (2002).
14. E. K. Payne, K. L. Shuford, S. Park, G. C. Schatz, and C. A. Mirkin, J. Phys. Chem. B **110**, 2150 (2006).
15. P. K. Jain, S. Eustis, and M. A. El-Sayed, J. Phys. Chem. B **110**, 18243 (2006).
16. B. Willingham, D. W. Brandl, and P. Nordlander, Appl. Phys. B **93**, 209 (2008).
17. E. D. Palik, *Handbook of Optical Constants of Solids* (Academic, 1985).
18. D. Weber, P. Albella, P. Alonso-Gonzalez, F. Neubrech, H. Gui, T. Nagao, R. Hillenbrand, J. Aizpurua, and A. Pucci, Opt. Express **19**, 15047 (2011).
19. N. Dubrovina, L. O. Cunff, N. Burokur, R. Ghasemi, A. Degiron, A. Lustrac, A. Vial, G. Lerondel, and A. Lupu, Appl. Phys. A **109**, 901 (2012).
20. T. V. Teperik and A. Degiron, Phys. Rev. Lett. **108**, 147401 (2012).
21. B. Lamprecht, G. Schider, R. T. Lechner, H. Ditlbacher, J. R. Krenn, A. Leitner, and F. R. Aussenegg, Phys. Rev. Lett. **84**, 4721 (2000).
22. D. P. Fromm, A. Sundaramurthy, P. J. Schuck, G. Kino, and W. E. Moerner, Nano Lett. **4**, 957 (2004).